Separation and Purification Technology 287 (2022) 120590

Contents lists available at ScienceDirect

Separation and Purification Technology

journal homepage: www.elsevier.com/locate/seppur

An elution-based method for estimating efficiencies of aerosol collection devices not affected by their pressure drops

Yi-Bo Zhao [a,b], Tianyu Cen [c,d], Jiukai Tang [a,b], Weidong He [a,b,e], Christian Ludwig [c,d], Sheng-Chieh Chen [f], Jing Wang [a,b,*]

[a] Institute of Environmental Engineering, ETH Zürich, Zürich 8093, Switzerland
[b] Advanced Analytical Technologies, Empa, Ueberlandstrasse 129, Dübendorf 8600, Switzerland
[c] Environmental Engineering Institute (IIE, GR-LUD), School of Architecture, Civil and Environmental Engineering (ENAC), École Polytechnique Fédérale de Lausanne (EPFL), Lausanne 1015, Switzerland
[d] Bioenergy and Catalysis Laboratory (LBK-CPM), Energy and Environment Research Division (ENE), Paul Scherrer Institut (PSI), Villigen PSI 5232, Switzerland
[e] Filter Test Center, School of Resources and Civil Engineering, Northeastern University, NO. 3-11, Wenhua Road, Heping District, Shenyang Liaoning 110819, China
[f] Department of Mechanical and Nuclear Engineering, Virginia Commonwealth University, 401 West Main St., Richmond, VA 23284, USA

ARTICLE INFO

Keywords:
Elution
NaCl
Collection efficiency
Aerosol sampler
Pressure drop
Size redistribution

ABSTRACT

The evaluation of collection efficiencies of aerosol samplers becomes challenging with high pressure drops. The evaluation approaches applied at various conditions deserve further development, especially when a high pressure drop is induced by the sampler. In this work, an elution-based method using NaCl aerosol was proposed to estimate the size-resolved collection efficiency which was not affected by the pressure drop. More specifically, a Condensation Particle Counter (CPC) was used to count the upstream particle number, and the collected NaCl particles were eluted and determined by Inductively Coupled Plasma Mass Spectrometry (ICP-MS) for estimating the collected particle number. The relationship between number-based concentration and mass-based concentration of NaCl particles was established. A stainless steel impactor for Differential Mobility Analyzer (DMA), polydimethylsiloxane (PDMS)-based microchannel, and a homemade impactor containing 151 nozzles with a diameter of 0.1 mm were employed to investigate the feasibility of the elution method. DMA-selected particles with a nominal size are considered to be the monodisperse aerosol, which was commonly used for estimating the collection efficiencies of samplers, but size redistribution of downstream monodisperse aerosol with the particle size smaller than 100 nm and larger than the cutoff size (D_{50}) was revealed through the elution method, which affected the collection efficiency measured by either conventional CPC- or elution-based method. It was found that the elution method was dependent on the D_{50} value of the sampler, and the applicable size range was from 100 nm to D_{50} (D_{50} < 500 nm) or from 100 nm to 500 nm (D_{50} greater than 500 nm). This study provided insights into the size-dependent particle transport through aerosol samplers, and the development of an elution-based method to estimate pressure drop-independent collection efficiencies.

1. Introduction

Aerosol samplers such as impactors, impingers, and cyclones are widely used to collect or classify airborne particles [1]. To evaluate the aerosol samplers, its size-resolved collection efficiency is normally investigated. The online aerosol instruments such as the scanning mobility particle sizer (SMPS) or aerodynamic particle sizer (APS) are often employed to measure the upstream (N_{up}) and downstream (N_{down}) particle number concentrations of the samplers to determine the collection efficiency (η_P) [2]:

$$\eta_P = \frac{N_{up} - N_{down}}{N_{up}} \quad (1)$$

However, obtaining an accurate particle size and number concentration becomes challenging when the inlet pressure of the online instruments is outside the operating range due to the high pressure drop induced by samplers [3]. For example, Condensation Particle Counter (CPC) 3775 could operate normally only at an inlet pressure of 0.75 to 1.05 atm [4]. Under a low pressure condition (e.g. 0.5 atm), the counting efficiency of a CPC can be largely reduced due to the particle diffusion

* Corresponding author.
E-mail address: jing.wang@ifu.baug.ethz.ch (J. Wang).

https://doi.org/10.1016/j.seppur.2022.120590
Received 8 December 2021; Received in revised form 17 January 2022; Accepted 26 January 2022
Available online 30 January 2022

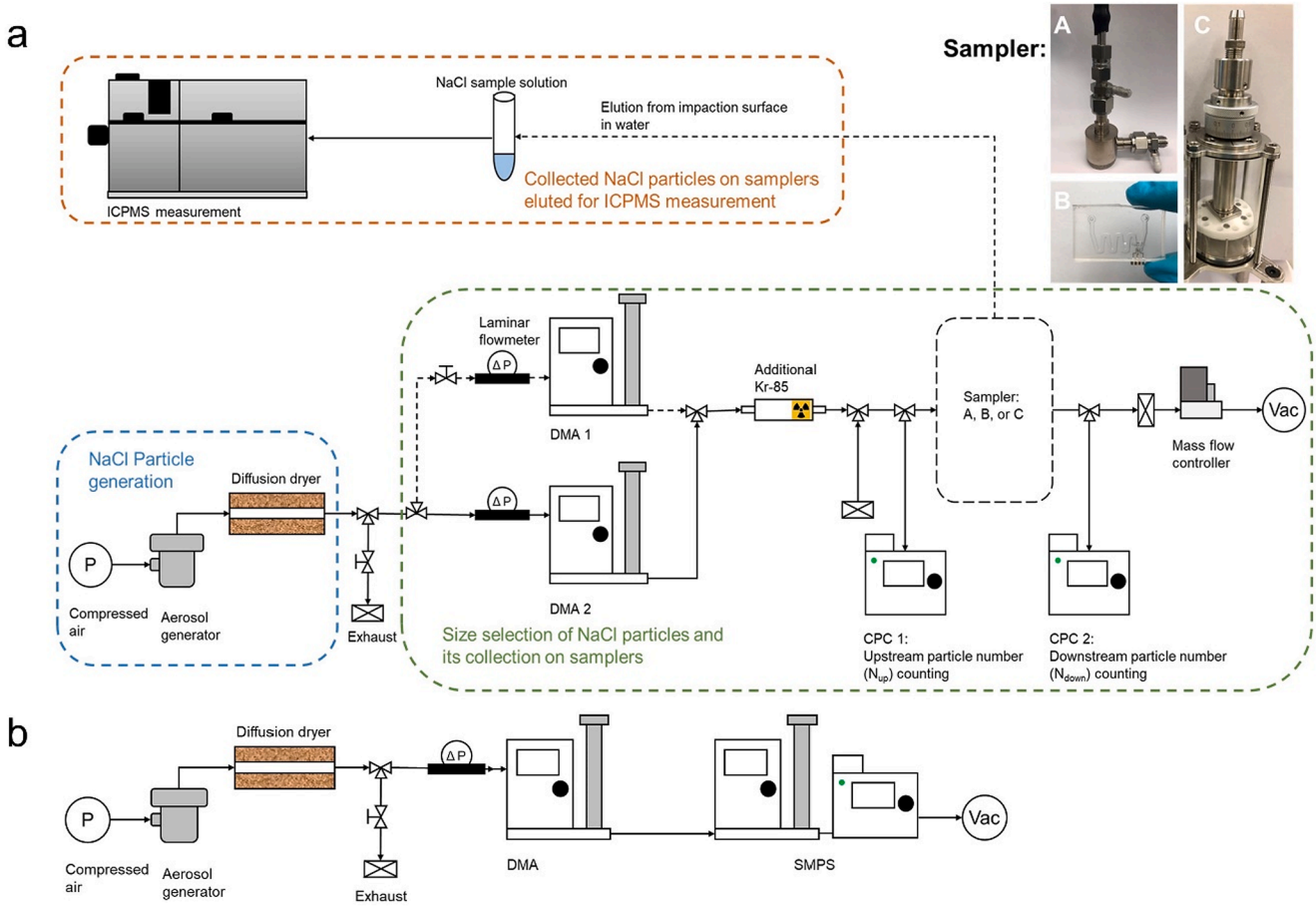

Fig. 1. Setup schematic of (a) collection efficiency evaluation and (b) size distribution determination using SMPS for monodisperse particles. Dash lines for DMA mean the optional connections. Sampler A, B and C represent the metal-based impactor for DMA, PDMS-based microchannel and homemade impactor, respectively.

loss for small particles and lower particle growth rates by the butanol condensation [5–7].

To alleviate the problem of the collection efficiency measurement affected by a high pressure drop, some instrumental modifications with additional devices for online particle counting have been made. For example, a pressure reducer was built to balance the pressure drop between upstream and downstream, so that the aerodynamic particle size spectrometer was able to work at a pressure drop as high as 0.5 atm [5]. A modification in the sampling line with a foil bag was made to allow the operation of SMPS at a low pressure [8]. A sample extractor with the piston arrangement is applied to reach the pressure equilibration required by APS and SMPS [9]. A Differential Mobility Particle Sizer (DMPS) system for low-pressure and low-temperature application was developed, which was able to work in the pressure range of 100 – 1000 hPa [10]. A modified CPC 7610 with a pressure equalizing tube was employed to measure particle concentration at pressures as low as 160 hPa [11]. More recently, a commercial low-pressure ejector has been investigated in a pressure range of 20 – 180 mbar and size range of 15 – 80 nm [12,13]. TSI model 3068 electrometer or Keithley model 6514 electrometer are alternative ways to estimate the downstream particle number by measuring electric currents under low pressure conditions [14,15], however, the charging status of the particles needs to be well controlled.

Besides the online instrumental counting, elution-based methods such as fluorometric techniques were used to estimate the collection efficiency [16]. Fluorescein labelled aerosol were collected and eluted into a solution, and then the fluorescein intensity was analyzed by a fluorometer. For example, oleic acid particles containing the uranine dye tracer were used to determine the collection efficiency of the Electrical Low-Pressure Impactor [17]. Fluorescence polystyrene microspheres were also employed to estimate the collection efficiency by elution and counting [18,19], but the elution efficiency could vary from 50 % to 100 % [20], which might result in an inaccurate estimation of the collection efficiency. Highly hydrophilic ammonium fluorescein particles were also used for estimating the collection efficiency and particle loss of a designed particle-into-liquid sampler [21]. The main disadvantage of the fluorometric method is that fluorescence is not specific and fades quickly [22]. The application of the fluorometric method is mainly limited by the fixed sizes of fluorescein insoluble particles, while estimation of collection efficiency in terms of particle number remains uncertain using mass concentrations of soluble fluorescein particles generated from a liquid solution.

Besides fluorometric techniques and modifications of online instrumental counting, it is beneficial to develop an alternative method that estimates the collection efficiency of samplers in a simple and reliable manner in a tunable size range, and is not affected by the pressure drop. Many common aerosol samplers are made out of metal, and polydimethylsiloxane (PDMS) is becoming more widely used in the fabrication of miniaturized aerosol sampling units [23]. In this study, an elution-based method using NaCl particles was developed and examined using metal- and PDMS-based aerosol samplers, and a homemade impactor. Upstream CPC particle number and ICPMS-measured Na concentration of collected particles were analyzed to address the downstream CPC operation issue at high pressure drops and to calculate the collection efficiency. On one hand, with this method, ICP-MS was introduced for estimating the collection efficiency of samplers under high pressure drop to avoid the incompetence or modification of the online instruments such as CPC, SMPS and APS. On the other hand, this

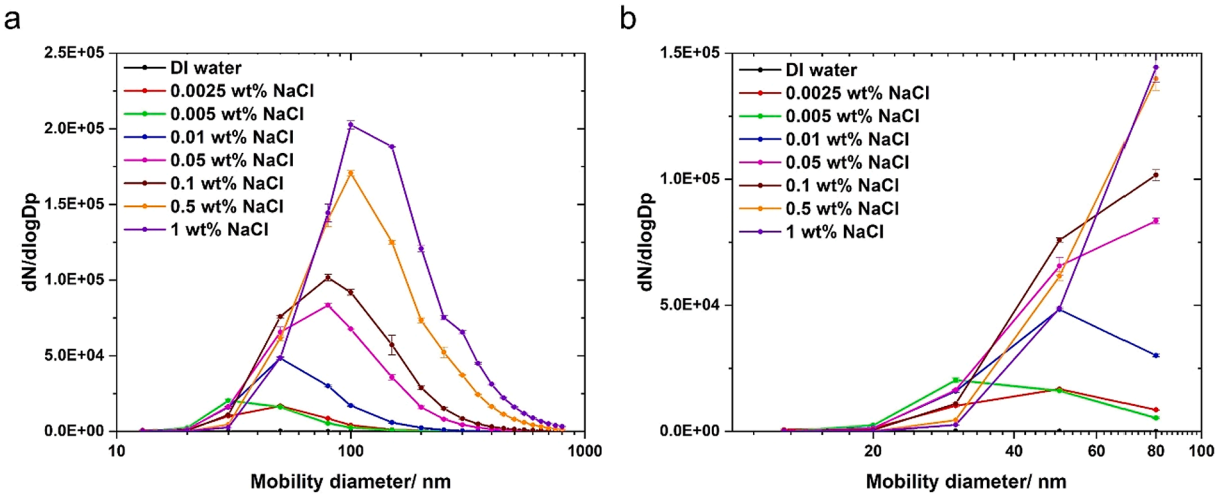

Fig. 2. Relationship between NaCl solution concentration (0.0025, 0.005, 0.01, 0.05, 0.1, 0.5 and 1 wt%) and generated particle number concentration in the size range of (a) 13 – 800 nm and (b) 13 – 80 nm in terms of electrical mobility diameter at 2.8 bar.

study also extended the application of the elution-based methods to investigate the size-resolved particle transport through samplers.

2. Materials and methods

2.1. Generation of the NaCl aerosol

Particle candidates such as NaCl [24], KCl, dust [25,26], SiO_2 [27], Polystyrene Latex Beads (PSL) [28], Di-Ethyl-Hexyl-Sebacat (DEHS) and silver nanoparticles [29] are widely used as the challenge particles in evaluating the collection efficiencies of samplers. Herein, NaCl solution was used to generate NaCl particles from a homemade atomizer at 2.8 bar with a flow rate of 3.8 L/min. Two Differential Mobility Analyzers (DMA 3080 and 3082, TSI) were used in parallel (Fig. 1) to generate a sufficient number of monodisperse NaCl particles smaller than 100 nm (aerosol flow: sheath flow = 1: 10), while one DMA (3082) was used for generating the particles larger than 100 nm. The aerosol flow was kept the same for the two DMAs used for particles smaller than 100 nm. The size selection of the DMA was confirmed using 310 nm polystyrene latex (PSL) particles (Fig. S1). An additional neutralizer after the DMA was installed to neutralize the monodisperse particles and to minimize the filtration efficiency induced by electrostatic forces (i.e. particle losses) [29]. In this work, monodisperse particles were defined as the DMA-selected particles with a nominal size. The aerosol inflow to the DMA was 0.6 and 0.3 L/min for classifying particles smaller and larger than 400 nm, respectively (Fig. 1). The aerosol flow was kept same (0.6 L/min) for the two DMA used for particles smaller than 100 nm. The collection time was adjusted to ensure sufficiently high particle concentration, which was prepared as ppb-level elution sample and measured by ICP-MS. In this study, 30, 50, 80, 100, 200, 300, 400, 500, 600, 700, 800 nm particles were collected for 16 h, 8 h, 2 h, 80 min, 40 min, 20 min, 20 min, 20 min, 20 min, 20 min, 20 min, respectively. A conventional impactor with a nozzle diameter of 0.0710 cm for DMA 3080 [30] and a designed PDMS microchannel [31] were used in this study to develop and validate the estimation method. To reduce the particle bouncing, Tween 20 viscous liquid (Sigma-Aldrich) was used to coat the surface of the impactor [32,33], which is miscible in water. All tubing was rinsed with Milli-Q water in an ultrasonic bath to avoid any contamination from tubing. Particle numbers of specific sizes counted by the upstream and downstream CPCs were corrected by dummy measurements, i.e., the particle sampler was replaced by a short empty tube and all the other parts of the setup stayed the same. Then the ratio of particle number concentration counted by upstream and downstream CPCs was obtained to correct the CPC-counted upstream particle number concentration. The result showed that the typical ratio of particle numbers was lower than 1 for the particles in the size range of 50 – 300 nm (Fig. S2). In detail, the lowest ratio was around 0.8 for about 100 nm particles.

According to the relationship between NaCl solution concentrations and generated particle numbers shown in Fig. 2, 0.05 wt% was used to generate particles smaller than 50 nm, while 1 wt% was used to generate particles larger than 50 nm, to maximize the generated particle number. The results indicated that the water residuals in the aerosol accounted for<0.5 % of the total particle volume using 0.05 and 1 wt% NaCl solutions. Therefore, it was reasonable to assume that the fraction of impurities in NaCl particles was negligible. The collected NaCl particles smaller than 100 nm and larger than 100 nm were eluted by MiliQ water as 5 and 10 mL samples in centrifuge tubes, respectively, and 1 % HNO_3 (Supelco, Suprapur) was added prior to ICPMS measurements. The dissolution of the NaCl particles collected from samplers was affected by particle sizes and mass concentrations. For example, small particles and low mass concentrations could lead to relatively insufficient elution process. The effects of these factors were further discussed in section 3.4. The conversion of particle number to the corresponding mass concentration in water is based on the following equation:

$$\frac{C_P = N_P \bullet 0.4 \bullet V_P \bullet \rho_P}{V_{sample}} \quad (2)$$

where N_P is the total NaCl particle number, C_P is the NaCl mass concentration in water (μg/L),V_{sample} is the volume of the liquid sample (mL), 0.4 is the mass fraction of sodium in NaCl, V_P is the volume of a single NaCl particle (assuming a spherical particle with a nominal mobility diameter), ρ_P is the density of NaCl particle (assuming 2.16 g/cm^3 [34]). It is noted that the results derived from equation (2) are also affected by various factors, such as particle shape and particle diameters used in the equation. For example, the relationship between aerodynamic and geometric diameters is based on the ratio of the square root of slip correction of these two diameters [35], and dynamic shape factor and particle density are involved to convert mobility diameter into aerodynamic diameter [36]. In this work, CPC-counted collection efficiency (η_{CPC}) refers to equation (1). And the calculated collection efficiency (η_{cal}) is based on the following equation:

$$\eta_{cal} = \frac{C_{ICP}}{C_{up}} \quad (3)$$

where C_{ICP} is the Na concentration derived from ICP-MS measurements, and C_{up} is the mass concentration of Na in upstream particles calculated

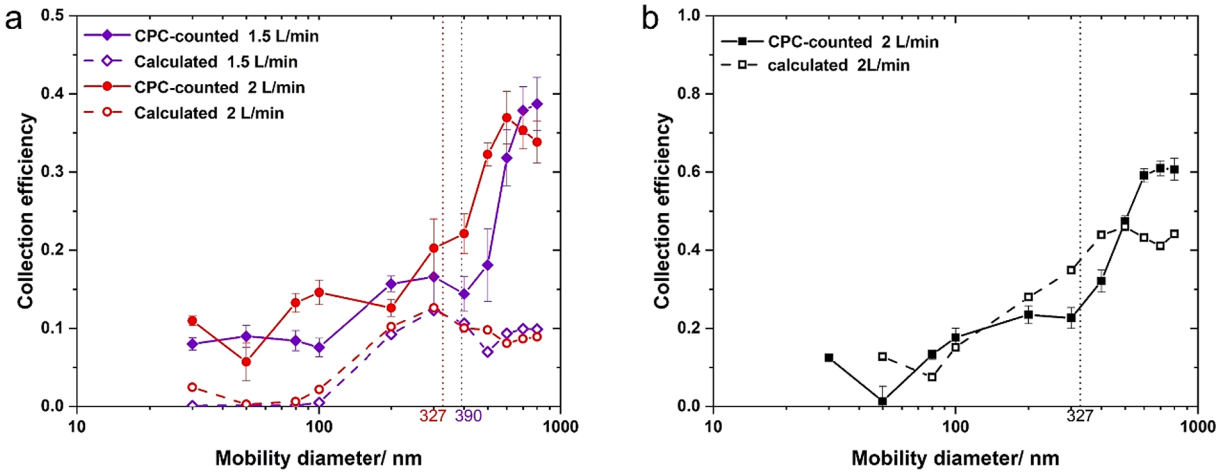

Fig. 3. Experimental and calculated collection efficiency of NaCl particles in the impactor for DMA (a) without and (b) with Tween 20 coating at 1.5 and 2 L/min. Vertical dash lines indicate the cutoff diameter at the applied flow rates.

by equation (2).

2.2. Design and fabrication of the microchannel collector and the homemade impactor

A microchannel with a cross section area (1.6 mm × 1.6 mm) was used to investigate the feasibility of the elution-based method (Fig. S3). The detailed description of the microchannel was reported in the previous study [31]. The ratio of the radius of curvature to the microchannel diameter was 2 [20]. The microchannel mold was designed using Auto CAD and printed using a 3D printer. PDMS monomer (Sylgard 184, Dow Corning, Midland, USA) was mixed with curing agent in the volume ratio of 10:1, and then degassed in a vacuum desiccator. The PDMS gels were subsequently cast onto the mold and peeled off after being heated at 70 °C for four hours, and these PDMS peelings were bound after plasma treatment. The schematic of the microchannel is shown in Fig. S3.

The homemade impactor consisted of stainless steel tubing and cover, Polytetrafluoroethylene (PTFE) mounting plate with an aluminum foil as the impaction plate, and glass wall (Fig. S4). It was noted that some parts such as the inner wall were not metal-based materials, which could cause particle loss. The homemade impactor containing 151 nozzles with a diameter of 0.1 mm at 6.4 L/min resulted in a cutoff size of 74 nm in terms of NaCl particles.

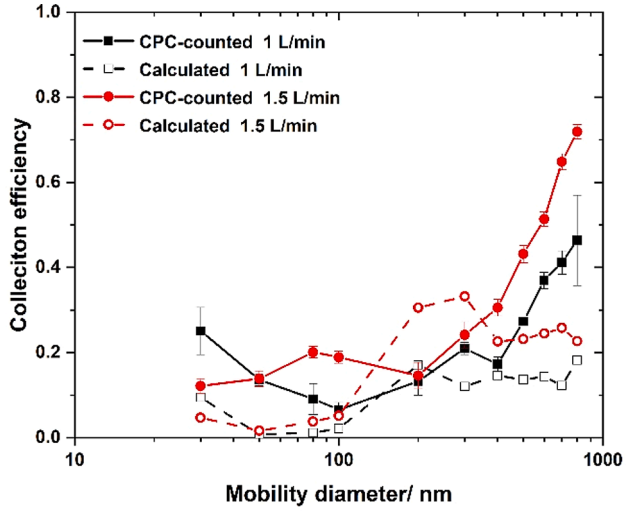

Fig. 4. Experimental and calculated collection efficiency of NaCl particles in the microchannel at 1 and 1.5 L/min.

2.3. Theory

The cutoff diameter of the impactor is defined as the following [30]:

$$D_{50} = \sqrt{\frac{9\pi Stk\mu W^3}{4\rho_P C_c Q}} \tag{4}$$

where D_{50} is the cutoff diameter, *Stk* is the cut-off Stokes number, which is 0.23, μ is the gas viscosity (g/(cm·s)),*W* is the nozzle diameter (cm), ρ_P is the particle density (g/cm^3) , *Q* is the volumetric flow rate (cm^3/s), C_c is the Cunningham Slip Correction according to the following equation [37]:

$$C_c = 1 + \frac{p_0\lambda_0}{pD_P}\left[2.34 + 1.05\exp\left(-0.39\frac{pD_P}{p_0\lambda_0}\right)\right] \tag{5}$$

where p_0 is the pressure at the reference state (pa), λ_0 is mean free path at the reference state (nm), *p* is the pressure (pa), and D_P is the particle diameter (nm).

2.4. Mass size distribution of monodisperse NaCl aerosol

The NanoMOUDI 122NR is a well-designed sampler, which has the stage cut-sizes of 10000, 5600, 3200, 1800, 1000, 560, 320, 180, 100, 56, 32, 18, and 10 nm at a sampling flow rate of 30 L/min [38]. It was used to determine the mass size distribution of monodisperse NaCl particles and examine if the elution-based method is applicable for multiple-stage impactors. In the experiment, particles were collected on aluminum foils at a flow rate of 26.0 – 26.5 L/min. DMA configuration and flow concept were the same as described above to generate monodisperse NaCl particles. Monodisperse particles with the mobility diameter of 50, 100, 300, 500, 600, and 700 nm were generated for 11 h, 3 h, 1 h, 1 h, 1 h, and 1 h, respectively. Particle samples were eluted using Mili-Q water from aluminum foils on impaction stages.

3. Results and discussion

3.1. Collection efficiency of the impactor and the microchannel collector

The theoretical cutoff diameters were 315 and 375 nm at 2 and 1.5 L/min of the impactor calculated by equation (4), respectively (Fig. 3a). Considering the shape factor of 1.08 [39–41], the corrected electrical mobility diameters were 327 and 390 nm for the theoretical cutoff diameter, respectively. However, the experimental cutoff diameters at 2

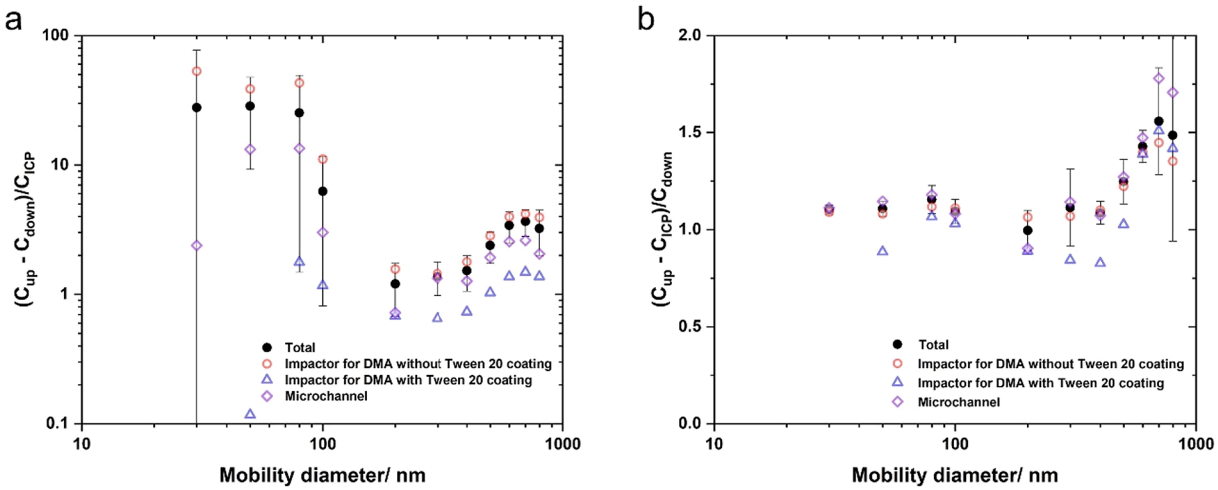

Fig. 5. (a) Ratio of size-resolved CPC-counted to the calculated collected particle concentration, and (b) ratio of calculated to CPC-counted downstream particle concentration. Total is the average of the microchannel and the impactor without Tween 20 coating.

and 1.5 L/min were larger than 600 nm (Fig. 3a), which indicated the significant solid particle bouncing on metal surface [42]. The collection efficiency for 1000 nm NaCl at 1.5 L/min and 2 L/min was 50.9 ± 5.7 % and 33.5 ± 15.2 %, respectively. The collection efficiency was lower with a higher velocity due to the increasing fraction of bounce [43]. Previous studies showed that particle bouncing was likely to occur on designed impactors when the particle was larger than 200 nm [44,45]. In contrast, the collection efficiency of Tween 20 coated impactor at 2 L/min was improved and the experimental cutoff diameter was about 400 nm (Fig. 3b). It demonstrated that Tween 20 was capable of reducing the particle bouncing and facilitating the estimation of actual collection efficiency with the elution-based method (Fig. 3b). The calculated collection efficiency based on the elution-based method indicated the underestimation of the performance of particle collection (Fig. 3a). In comparison with the impactor without the Tween 20 coating layer, the calculated collection efficiency with the Tween 20 coating layer agreed better with the CPC-counted collection efficiency (Fig. 3b).

The microchannel was a W-shape particle collector, and employed to collect particles under inertial force. The cutoff diameters of the microchannel at 1 and 1.5 L/min were about 800 and 500 nm, respectively (Fig. 4). Similarly, without Tween 20 coating layer, the calculated collection efficiency of the microchannel diverged from the CPC-counted collection efficiency, especially in the size range of 500 – 800 nm. As shown in Fig. S5, particle loss and particle bouncing due to lower particle number and larger particles size were the main factors to affect the collection efficiency in the size range of 500 – 800 nm.

3.2. Comparison of CPC-counted and calculated collection efficiencies and downstream particle concentrations

Fig. 5 showed the ratio of collected and downstream particle concentration. Here, the ratio of the collected concentration was defined $(C_{up} - C_{down})/C_{ICP}$, and the ratio of the downstream particle concentration was $(C_{up} - C_{ICP})/C_{down}$. The ratio of the collected particle concentration without Tween 20 coating indicated possible particle mass loss in the size range of 30 – 100 and 500 – 800 nm (Fig. 5a), because the collected particle mass concentration obtained by ICP-MS measurements was lower. Compared to the ratio on the PDMS-based microchannel, the ratio of the collected particle concentration on the metal-based impactor was higher by 3.27 times in the size range of 50 – 100 nm, and it was 22.2 times higher in terms of 30 nm particles (Fig. 5a). It demonstrated that smaller particles diffused with a high diffusivity [46] and stuck to interior wall or impaction surface of the impactor during particle transport, which caused particle loss and changes of size distribution of monodisperse particles. In particular, the lower ratios of the collected particle concentration for the microchannel than those for the impactor suggested the particle loss on the interior wall especially for the particles smaller than 100 nm (Fig. S5a). Therefore, the actual collection efficiency of small particles in the size range of 30 – 100 nm was likely to be lower than the CPC-counted collection efficiency shown in Fig. 5a and 5b. A previous study also elaborated that spontaneous particle loss occurs during the particle collection [19].

Besides that, elution efficiency played an important role for the ratio being over 1, which was discussed in more details in section 3.4. The actual geometric diameter is larger than the nominal geometric diameter

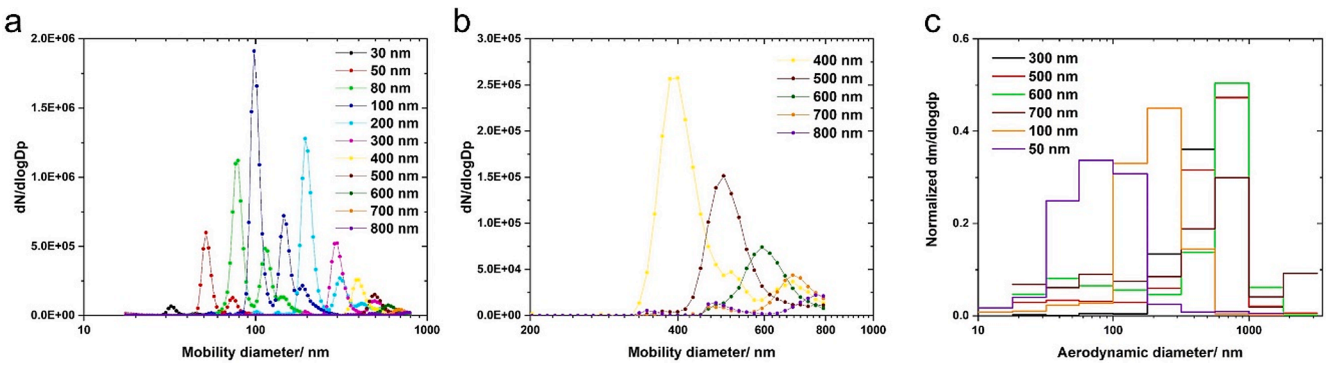

Fig. 6. Size distribution of the monodisperse (a) 30 – 800 nm and (b) 400 – 800 nm NaCl particles, (c) mass size distribution of monodisperse NaCl in terms of aerodynamic diameter.

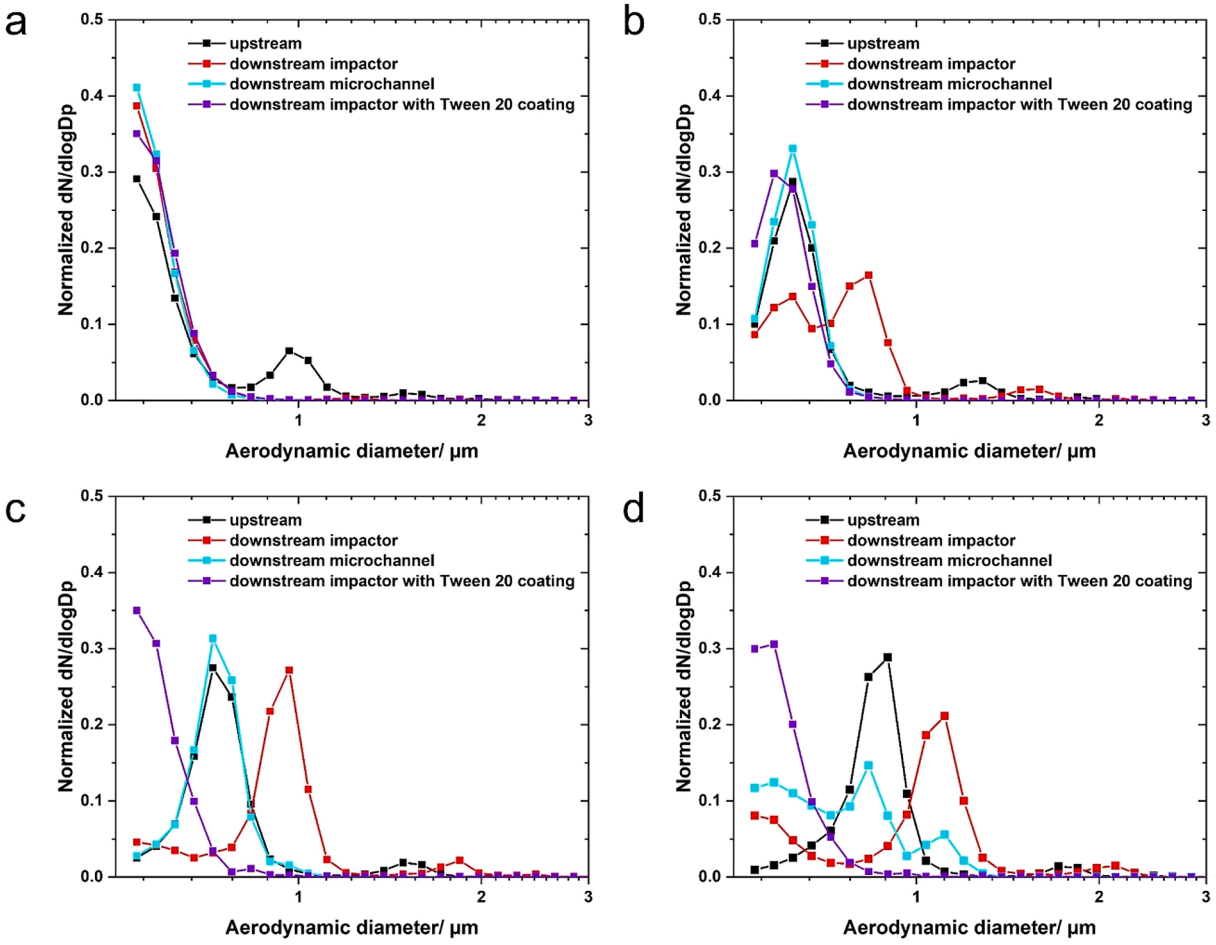

Fig. 7. Size distribution of upstream and downstream impactor for DMA and microchannel in terms of aerodynamic diameter at 1.5 L/min with monodisperse (a) 500, (b) 600, (c) 700, and (d) 800 nm NaCl selected by DMA.

we used in the conversion equation according to the size distribution determined by SMPS (Fig. 6a and b), which could lead to a ratio of lower than 1. Nonetheless, the downstream particle concentration ratio in the size range of 30 – 500 nm was close to 1. More specifically, the downstream particle concentration ratio without Tween 20 coating was 0.94 ± 0.10 with the particle smaller than 500 nm. It implied that particle loss and changes of size distribution of monodisperse particles had a minor effect on the estimation of collection efficiency using the elution-based method, provided the theoretical collection efficiency was lower than 50 %. The theoretical collection efficiency of 50 % was determined based on the equation of cutoff size.

The discrepancy between CPC-counted concentration and calculated concentration was becoming evident with particles larger than 500 nm (Fig. 5a and b). It was likely due to the change of size distributions of upstream and downstream monodisperse large particle, which affected the actual average geometric diameter. According to the size distribution of monodisperse particles shown in Fig. 6a and b, the defined particle diameter was not the only size in monodisperse particles. In detail, the lower limit of the particle diameter of the monodisperse NaCl particles (when the particle concentration approached 0) was 82.9 ± 7.2 % and 30.2 ± 1.4 % of the defined monodisperse diameter in the range of 30 – 300 nm and 500 – 800 nm respectively, indicating a broader size range of monodisperse particles of 500 – 800 nm. It was more convenient to change the average geometric diameter by altering the size distribution of downstream monodisperse particles in the size range of 500 – 800 nm through particle bouncing. The mass distribution determined by Nano MOUDI also confirmed the wide range of monodisperse NaCl particles selected by DMA (Fig. 6c). For example, 50 nm and 500 nm monodisperse NaCl particles distribute in the aerodynamic diameter range of 32 – 180 nm and 320 – 1000 nm, respectively. It also indicated that the elution-based method was applicable for single-stage samplers rather than multiple-stage samplers, since it would be unpredictable to convert mass concentration into particle number, considering possible size redistribution of monodisperse NaCl particles.

Despite the variation of concentration ratios as a function of particle size, the limited difference between the average downstream concentration ratio on the impactor and microchannel implied that different materials had a limited effect on the estimation of downstream concentration (Fig. 5b). However, the elution efficiency from the PDMS surface was not consistent in the size range of 700 – 800 nm (Fig. S5b). According to the size distribution of monodisperse NaCl aerosol upstream and downstream impactor and microchannel (Fig. 7), particle bouncing on the impactor was clearly observed with the particle size larger than 500 nm as the fraction of large particles was larger compared to the upstream size distribution. It implies that other elution methods such as fluorometric method with highly hydrophilic fluorescein particles, are also not applicable for aerosol samplers with particle bouncing in large particle size ranges. It was also confirmed by a previous study that the collection efficiency of Berner impactor was much lower especially with the particle size larger than cutoff size, evaluated by using ammonium fluorescein particles due to the particle bounce from the substrate [47]. In contrast, no significant change of size distribution in the downstream microchannel was observed.

Air flow leaves an oil-free area on the impaction plate facing the orifice, and the pores of the metal plate act as oil reservoirs [44]. The Tween 20 coating layer could stabilize the ratio of collected particle

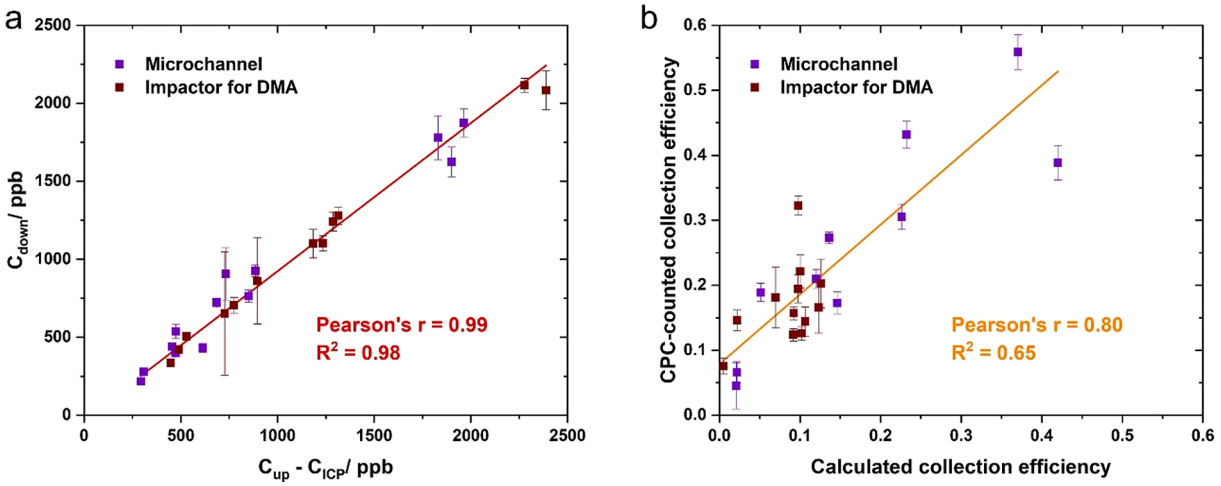

Fig. 8. Global relationship between the calculated and CPC-counted (a) downstream particle concentration, and (b) collection efficiency of the impactor and the microchannel in the size range of 100 – 500 nm.

concentration and downstream concentration to 0.97 ± 0.34 and 1.00 ± 0.22 in the size range of 80 – 800 nm. Moreover, it prevented the particle bouncing and might also change the geometric structure of the impaction plate to form a curved rather than flat metal surface used and therefore can collect more particles, which is similar to an additional punched impaction plate used to increase the collection efficiency [48]. Nonetheless, the ratio of concentration of collected particles on impaction plate and downstream concentration was lower than 1 in the size range of 30 – 50 nm and 200 – 400 nm, as a result of higher ICP-MS result (C_{ICP}). The main reason was that Na concentration in the pure Tween 20 solution measured by ICP-MS was 366 ± 11 ppm, which was high enough to increase the Na concentration in the elution samples. The volume of Tween 20 used for a coating layer was on a microliter level (e.g. 5 μL), so a slight variation of the added volume could lead to a different concentration of Na, making it difficult to subtract concentrations of Na in the Tween 20 from ICP-MS validated concentrations. Tween 20 coating layer also led to a slight reaerosolization and higher downstream particle counting by generating 28.8 ± 4.3 particles per cm^3 (Fig. S6). Therefore, coating solutions such as Tween 20 containing Na were not recommended to be applied for the elution-based method.

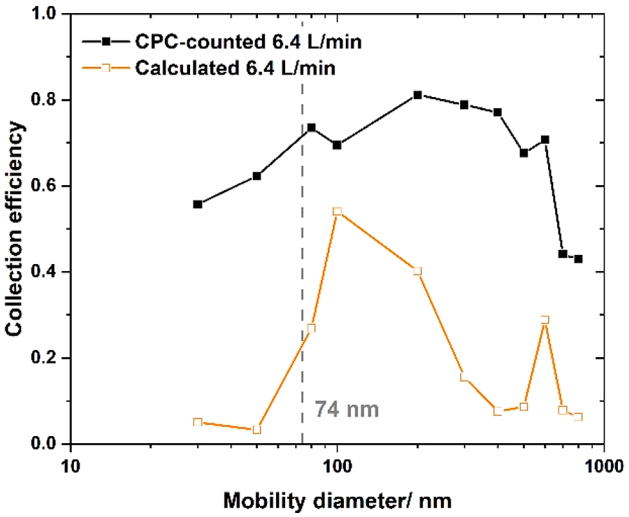

Fig. 9. Experimental and calculated collection efficiency of NaCl particles in the homemade impactor at 6.4 L/min.

3.3. Size redistribution of the downstream monodisperse aerosol

In average, the ratios of the CPC-counted collected particle number to the calculated particle number derived from ICPMS verified concentration were above 10 and 2 in the size range of 30 – 100 and 500 – 800 nm, respectively (Fig. 5a). Particle diffusion of small particles and particle bouncing of large particles led to the size redistribution, which increased the actual average geometric diameter of monodisperse NaCl aerosols by depositing smaller particles on the impaction plate. APS-measured aerodynamic diameters of upstream and downstream impactor indicated an increasing geometric diameter of monodisperse 600, 700 and 800 nm particles by 12.8 % at 1.5 L/min (Table S1). It was noted that the sizing accuracy of APS was affected by unit-to-unit variability (up to 10 % deviation) and the number of resolved bins [49], which could cause the difference between the measured aerodynamic diameter and that derived from the mobility diameter theoretically. APS results suggested that smaller particles in the monodisperse aerosol were captured by sampler, whereas larger particles left away likely due to particle bouncing, which confirmed the size redistribution of downstream aerosol in the range of 600 – 800 nm (Fig. 7). Here, the size redistribution was defined as the change in the normalized particle number as a function of particle sizes. In contrast, the ratio was close to 1 in the size range of 100 – 500 nm (Fig. 8a), which indicated a relatively consistent upstream and downstream size distribution when the theoretical collection efficiency was lower than 50 %. Good correlation between calculated and CPC-counted collection efficiency in the size range of 100 – 500 nm indicated the applicable range of the elution-based method (Fig. 8b). The non-zero intercept implied a minor effect of particle loss on the inner wall of samplers or sample loss during elution process, resulting in a higher CPC-counted collection efficiency compared to calculated collection efficiency.

3.4. The effect of cutoff size and elution efficiency on the elution-based method

As the result showed, the applicable size range possibly depended on the cutoff size of the single-stage sampler. More specifically, the cutoff size of the impactor and the microchannel were about 400 and 800 nm, respectively (Figs. 3 and 4), while the applicable size range was smaller than 500 nm. Therefore, a homemade impactor with a cutoff size of 74 nm was employed to investigate the effect of cutoff size on the method. Fig. 9 suggested that the collection efficiency of 100 nm NaCl particles was successfully estimated according to CPC-counted collection efficiencies, whereas collection efficiencies of other particle sizes were underestimated compared to CPC-counted collection efficiencies. It was

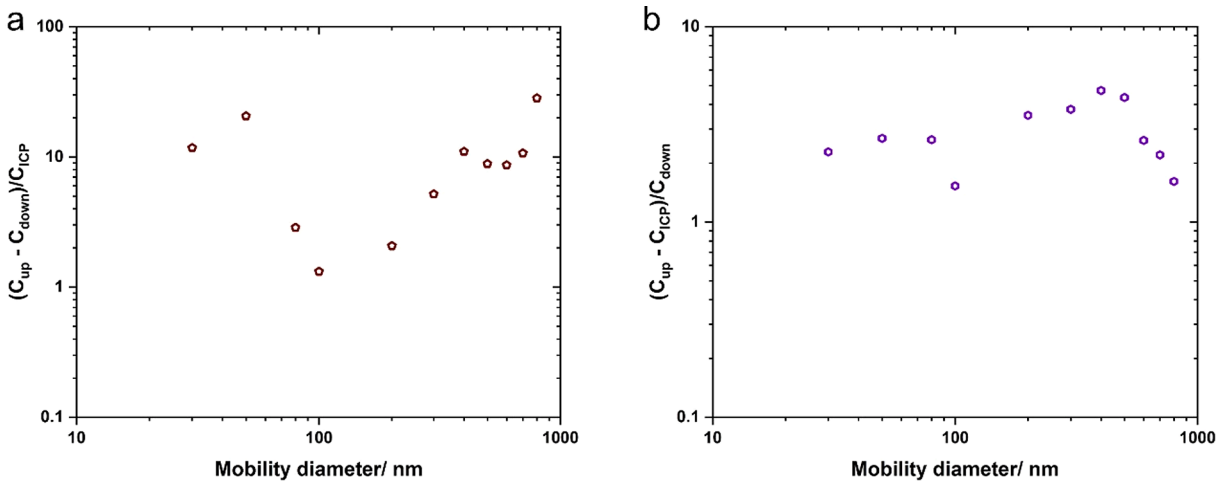

Fig. 10. (a) Average ratio of size-resolved CPC-counted to the calculated collected particle concentration, and (b) average ratio of calculated to CPC-counted downstream particle concentration using the homemade impactor at 6.4 L/min.

observed that the ratio of CPC-counted collected particle concentration to ICPMS concentration was 2 – 20 in the size range smaller than 100 nm (Fig. 10a), which indicated size redistribution remains similar with low or high collection efficiency. In contrast, the ratio of collected particle concentration was constant and close to 1 with 100 nm particles, which was close to the theoretical cutoff size of 74 nm. Similarly, the ratio of calculated to CPC-counted downstream particle concentration was close to 1 with 100 nm NaCl particles (Fig. 10b). The ratio of collected particle concentration and downstream particle concentration varied greatly in the size range of 600 – 800 nm (Fig. S7). It indicated that the elution method was associated with the cutoff size of samplers, which was found to be the upper limit of the size range of 100 – 500 nm.

To understand the role of elution efficiency in the elution-based method, the ratio of the collected particle concentration for the impactor, microchannel and homemade impactor were compared (Fig. 5a and 10a). The elution efficiency was mainly affected by the surface of the impaction plate, so we assumed a fixed elution efficiency as a function of particle size regardless of collection efficiencies. A similar ratio (~10) for the particle smaller 100 nm was observed, indicating a more significant role of elution efficiency over the size redistribution of downstream monodisperse particles, whereas the ratio was increasing from 2 to 10 with increasing collection efficiencies for the particles larger than 100 nm, which implied the size redistribution of downstream monodisperse particles dominated the changes of the ratio.

4. Conclusions

In this study, an elution-based method was proposed to estimate particle collection efficiency of samples regardless of pressure drops. Based on the correlation between CPC-counted and calculated collection efficiencies, CPC was used to measure the upstream particle number, and eluted samples from samplers were employed to estimate the collected particle concentration in the size range of 100 nm – D_{50} (D_{50} < 500 nm) or 100 – 500 nm (D_{50} greater than 500 nm). Nonetheless, the elution-based method might be applicable in a wider size range if a more monodisperse NaCl particles could be generated in future studies, especially for particles larger than 500 nm.

Size redistribution of monodisperse NaCl particles due to the diffusion of particles smaller than 100 nm and bouncing of particles larger than D_{50} or 500 nm were found to affect the estimation of collection efficiency. Specifically, elution efficiency played a more important role than size redistribution in the range of 30 – 100 nm and affected the estimated collection efficiencies, while size redistribution was more significant with a higher collection efficiency in the size range of 500 – 800 nm. In addition, size redistribution occurred with a collection efficiency of higher than 50 % in the size range of 100 – 500 nm. Thus, this method was also capable of investigating the transport and size redistribution of monodisperse particles through aerosol samplers. A more accurate conversion from particle number into mass concentration as a function of particle size can also be investigated to avoid the effects of the conversion and facilitate the particle transport studies using the elution-based method.

CRediT authorship contribution statement

Yi-Bo Zhao: Conceptualization, Methodology, Investigation, Writing – original draft. **Tianyu Cen:** Investigation, Resources, Formal analysis. **Jiukai Tang:** Investigation, Resources. **Weidong He:** Formal analysis, Data curation. **Christian Ludwig:** Validation, Formal analysis, Writing – review & editing. **Sheng-Chieh Chen:** Validation, Writing – review & editing. **Jing Wang:** Conceptualization, Resources, Writing – review & editing, Supervision.

Declaration of Competing Interest

The authors declare that they have no known competing financial interests or personal relationships that could have appeared to influence the work reported in this paper.

Acknowledgements

Y.-B. Zhao thanks the financial support from China Scholarship Council (CSC). T. Cen and C. Ludwig acknowledge the Swiss National Science Foundation for financial support (project 184817). We thank Daniel Rechenmacher for the drawing and manufacture of the homemade impactor.

Appendix A. Supplementary material

Supplementary data to this article can be found online at https://doi.org/10.1016/j.seppur.2022.120590.

References

[1] C.W. Haig, W.G. Mackay, J.T. Walker, C. Williams, Bioaerosol sampling: sampling mechanisms, bioefficiency and field studies, J. Hosp. Infect. 93 (2016) 242–255.
[2] J. Wang, P. Tronville, Toward standardized test methods to determine the effectiveness of filtration media against airborne nanoparticles, J. Nanopart. Res. 16 (2014) 2417.
[3] J. Kangasluoma, A. Franchin, J. Duplissy, L. Ahonen, F. Korhonen, M. Attoui, J. Mikkilä, K. Lehtipalo, J. Vanhanen, M. Kulmala, T. Petäjä, Operation of the Airmodus A11 nano Condensation Nucleus Counter at various inlet pressures and

various operation temperatures, and design of a new inlet system, Atmos Meas. Tech. 9 (7) (2016) 2977–2988.
[4] TSI corporation, Model 3775 Condensation Particle Counter Operation and Service Manual http://www.lisa.u-pec.fr/~formenti/Tools/Manuals/CPC-3775r-manual.pdf, 2007 (accessed March 2021).
[5] S.A. Grinshpun, K. Willeke, V. Ulevicius, A. Juozaitis, S. Terzieva, J. Donnelly, G. N. Stelma, K.P. Brenner, Effect of impaction, bounce and reaerosolization on the collection efficiency of impingers, Aerosol. Sci. Technol. 26 (4) (1997) 326–342.
[6] Z. Zhang, B.Y.H. Liu, Performance of TSI 3760 condensation nuclei counter at reduced pressures and flow rates, Aerosol. Sci. Technol. 15 (4) (1991) 228–238.
[7] M. He, S. Dhaniyala, M. Wagner, Characterization of filter performance under low-pressure operation, Aerosol. Sci. Technol. 50 (5) (2016) 417–428.
[8] F. Ober, M. Mayer, H. Büttner, F. Ebert, Aerosol measurement in low-pressure systems with standard scanning mobility particle sizers, Part. Part. Syst. Charact. 19 (4) (2002) 229–239.
[9] J.A. Hubbard, J.E. Brockmann, J. Dellinger, D.A. Lucero, A.L. Sanchez, B. L. Servantes, Fibrous filter efficiency and pressure drop in the viscous-inertial transition flow regime, Aerosol. Sci. Technol. 46 (2) (2012) 138–147.
[10] M. Seifert, R. Tiede, M. Schnaiter, C. Linke, O. Möhler, U. Schurath, J. Ström, Operation and performance of a differential mobility particle sizer and a TSI 3010 condensation particle counter at stratospheric temperatures and pressures, J. Aerosol. Sci. 35 (8) (2004) 981–993.
[11] M. Hermann, A. Wiedensohler, Counting efficiency of condensation particle counters at low-pressures with illustrative data from the upper troposphere, J. Aerosol. Sci. 32 (8) (2001) 975–991.
[12] T. Rosenberger, A. Münzer, D. Kiesler, H. Wiggers, F.E. Kruis, Ejector-based sampling from low-pressure aerosol reactors, J. Aerosol. Sci. 123 (2018) 105–115.
[13] T. Rosenberger, J. Neises, D. Kiesler, F.E. Kruis, Ejector-based nanoparticle sampling from pressures down to 20 mbar, J. Aerosol. Sci. 144 (2020) 105531.
[14] C.-J. Tsai, D.-R. Chen, H. Chein, S.-C. Chen, J.-L. Roth, Y.-D. Hsu, W. Li, P. Biswas, Theoretical and experimental study of an axial flow cyclone for fine particle removal in vacuum conditions, J. Aerosol. Sci. 35 (9) (2004) 1105–1118.
[15] S.-C. Chen, C.-J. Tsai, An axial flow cyclone to remove nanoparticles at low pressure conditions, J. Nanopart. Res. 9 (1) (2006) 71–83.
[16] J. Kesavan, R.W. Doherty, Use of Fluorescein in Aerosol Studies, in, Edgewood chemical biological center aberdeen proving ground md, 2000.
[17] M. Marjamäki, J. Keskinen, D.-R. Chen, D.Y.H. Pui, Performance evaluation of the electrical low-pressure impactor (ELPI), J. Aerosol. Sci. 31 (2) (2000) 249–261.
[18] D. Wang, M.M. Shafer, J.J. Schauer, C. Sioutas, A new technique for online measurement of total and water-soluble copper (Cu) in coarse particulate matter (PM), Environ. Pollut. 199 (2015) 227–234.
[19] K.S. Lim, K.W. Lee, Collection efficiency and particle loss of virtual impactors with different methods of increasing pressure drop, J. Aerosol. Sci. 37 (10) (2006) 1188–1197.
[20] I.V. Novosselov, R.A. Gorder, J.A. Van Amberg, P.C. Ariessohn, Design and performance of a low-cost micro-channel aerosol collector, Aerosol. Sci. Technol. 48 (8) (2014) 822–830.
[21] D. Wang, J. Jiang, J. Deng, Y. Li, J. Hao, A sampler for collecting fine particles into liquid suspensions, Aerosol. Air Qual. Res. (2020).
[22] J.P. Lodge Jr, Methods of air sampling and analysis, CRC Press, 1988.
[23] A.R. Metcalf, S. Narayan, C.S. Dutcher, A review of microfluidic concepts and applications for atmospheric aerosol science, Aerosol. Sci. Technol. 52 (3) (2018) 310–329.
[24] D.A. Japuntich, L.M. Franklin, D.Y. Pui, T.H. Kuehn, S.C. Kim, A.S. Viner, A comparison of two nano-sized particle air filtration tests in the diameter range of 10 to 400 nanometers, J. Nanopart. Res. 9 (1) (2006) 93–107.
[25] J.E. Yit, B.T. Chew, Y.H. Yau, A review of air filter test standards for particulate matter of general ventilation, Build. Services Eng. Res. Technol. 41 (6) (2020) 758–771.
[26] J.-H. Lim, S.-H. Oh, S. Kang, K.-J. Lee, S.-J. Yook, Development of cutoff size adjustable omnidirectional inlet cyclone separator, Separ. Purif. Technol. 276 (2021) 119397.
[27] G.-Y. Lin, L.-T. Cuc, W. Lu, C.-J. Tsai, H.-M. Chein, F.-T. Chang, High-efficiency wet electrocyclone for removing fine and nanosized particles, Separ. Purif. Technol. 114 (2013) 99–107.
[28] J.-H. Lim, D. Park, S.-J. Yook, Development of a multi-slit virtual impactor as a high-volume bio-aerosol sampler, Separ. Purif. Technol. 250 (2020) 117275.
[29] P. Sachinidou, Y.K. Bahk, M. Tang, N. Zhang, S.S.C. Chen, D.Y.H. Pui, B.A. Lima, G. Bosco, P. Tronville, T. Mosimann, M. Eriksson, J. Wang, Inter-laboratory validation of the method to determine the filtration efficiency for airborne particles in the 3–500 nm range and results sensitivity analysis, Aerosol. Air Qual. Res. 17 (11) (2017) 2669–2680.
[30] TSI corporation, Series 3080 Electrostatic Classifiers Operation and Service Manual. http://cires1.colorado.edu/jimenez-group/Manuals/SMPS_3080_manual.pdf, 2009 (accessed March 2021).
[31] Y.-B. Zhao, J. Tang, T. Cen, G. Qiu, W. He, F. Jiang, R. Yu, C. Ludwig, J. Wang, Integrated aerodynamic/electrochemical microsystem for collection and detection of nanogram-level airborne bioaccessible metals, Sensor. Actuator. B: Chem. 351 (2022) 130903.
[32] H.N. Phan, A.R. McFarland, Aerosol-to-hydrosol transfer stages for use in bioaerosol sampling, Aerosol. Sci. Technol. 38 (4) (2004) 300–310.
[33] S. Rodrigues, A. da Costa, N. Flórez-Fernández, M. Torres, M. Faleiro, F. Buttini, A. Grenha, Inhalable spray-dried chondroitin sulphate microparticles: effect of different solvents on particle properties and drug activity, Polymers 12 (2) (2020) 425.
[34] L. Morawska, G. Johnson, Z.D. Ristovski, V. Agranovski, Relation between particle mass and number for submicrometer airborne particles, Atmos. Environ. 33 (13) (1999) 1983–1990.
[35] O.R. Moss, Shape factors for airborne particles, Am. Ind. Hyg. Assoc. J. 32 (4) (1971) 221–229.
[36] W. Stöber, A note on the aerodynamic diameter and the mobility of non-spherical aerosol particles, J. Aerosol. Sci. 2 (4) (1971) 453–456.
[37] W.C. Hinds, Aerosol technology: properties, behavior, and measurement of airborne particles, John Wiley & Sons, 1999.
[38] Y. Yue, H. Chen, A. Setyan, M. Elser, M. Dietrich, J. Li, T. Zhang, X. Zhang, Y. Zheng, J. Wang, M. Yao, Size-resolved endotoxin and oxidative potential of ambient particles in Beijing and Zürich, Environ. Sci. Technol. 52 (12) (2018) 6816–6824.
[39] P.F. DeCarlo, J.G. Slowik, D.R. Worsnop, P. Davidovits, J.L. Jimenez, Particle morphology and density characterization by combined mobility and aerodynamic diameter measurements. part 1: theory, Aerosol Sci. Technol. 38 (12) (2004) 1185–1205.
[40] A. Khlystov, C. Stanier, S.N. Pandis, An algorithm for combining electrical mobility and aerodynamic size distributions data when measuring ambient aerosol special issue of aerosol science and technology on findings from the fine particulate matter supersites program, Aerosol. Sci. Technol. 38 (sup1) (2004) 229–238.
[41] Z. Wang, S.M. King, E. Freney, T. Rosenoern, M.L. Smith, Q. Chen, M. Kuwata, E. R. Lewis, U. Pöschl, W. Wang, P.R. Buseck, S.T. Martin, The dynamic shape factor of sodium chloride nanoparticles as regulated by drying rate, Aerosol. Sci. Technol. 44 (11) (2010) 939–953.
[42] J. Dirgo, D. Leith, Cyclone collection efficiency: comparison of experimental results with theoretical predictions, Aerosol. Sci. Technol. 4 (1985) 401–415.
[43] H.-C. Wang, W. John, Comparative bounce properties of particle materials, Aerosol. Sci. Technol. 7 (3) (1987) 285–299.
[44] C.-J. Tsai, C.-N. Liu, S.-M. Hung, S.-C. Chen, S.-N. Uang, Y.-S. Cheng, Y. Zhou, Novel active personal nanoparticle sampler for the exposure assessment of nanoparticles in workplaces, Environ. Sci. Technol. 46 (8) (2012) 4546–4552.
[45] C. Misra, S. Kim, S. Shen, C. Sioutas, A high flow rate, very low pressure drop impactor for inertial separation of ultrafine from accumulation mode particles, J. Aerosol. Sci. 33 (5) (2002) 735–752.
[46] M. Fierz, L. Scherrer, H. Burtscher, Real-time measurement of aerosol size distributions with an electrical diffusion battery, J. Aerosol. Sci. 33 (7) (2002) 1049–1060.
[47] R.E. Hillamo, E.I. Kauppinen, On the performance of the berner low pressure impactor, Aerosol. Sci. Technol. 14 (1) (1991) 33–47.
[48] T.-W. Cheon, J.-Y. Lee, J.-Y. Bae, S.-J. Yook, Enhancement of collection efficiency of an inertial impactor using an additional punched impaction plate, Aerosol. Air Qual. Res. 17 (10) (2017) 2349–2357.
[49] S. Pfeifer, T. Müller, K. Weinhold, N. Zikova, S. Martins dos Santos, A. Marinoni, O. F. Bischof, C. Kykal, L. Ries, F. Meinhardt, P. Aalto, N. Mihalopoulos, A. Wiedensohler, Intercomparison of 15 aerodynamic particle size spectrometers (APS 3321): uncertainties in particle sizing and number size distribution, Atmos. Meas. Tech. 9 (2016) 1545–1551.